Academic Journal of Science and Technology
ISSN: 2771-3032 | Vol. 11, No. 1, 2024

Effect of Hydrogen Embrittlement on Dislocation Emission from A Bifurcation Crack Tip in Nano-metallic Materials

Xiaoya Song, Min Yu

College of Civil Engineering, Central South University of Forestry and Technology, Changsha 410004, PR China

Abstract: A theoretical model was established to investigate the interaction between hydrogen clusters and edge dislocation near bifurcation crack tip in deformed nano-metallic materials. The model's solution was obtained by using the complex method, and the influence of hydrogen concentration, temperature, Relative crack length, material constants of nano-metallic materials and the dislocation emission angle on the critical stress intensity factor (SIFs) corresponding to the first dislocation emission from the crack tip was investigated through numerical analysis. The results show that dislocations are easy to emit from the crack tip at high hydrogen concentrations. However, under the influence of hydrogen clusters, the high temperature will make dislocation emission more difficult. At the same time, when relative cracks become longer, it becomes more difficult for dislocations to emit from the crack tip. As the angle of dislocation increased, the SIF first decreased and then increased. And as the angle between the main crack and the bifurcation crack continues to increase, the dislocation emission behavior at the tip of the bifurcation crack will be significantly promoted.

Keywords: Hydrogen clusters; complex variable method; dislocation emission; stress intensity factor; bifurcation cracks.

1. Introduction

Metals are commonly used materials in industry, and their mechanical properties can significantly affect their service life, which has received extensive attention from scholars. Grain size, as an important internal structural parameter of metallic materials, affects the mechanical properties of the materials. Especially, when the grain size of metallic materials is reduced to the nanometer order of magnitude, the mechanical properties of the materials will be significantly changed. In general, nano-metallic materials with a grain size of 100 nm or less are referred to as nano-metallic materials [1-3]. Cracks are very common in nano-metallic materials and there are many typical shapes of crack, such as surface semi-elliptical cracks, cross cracks, interfacial co-linear cracks, and elliptical blunt cracks. When the stress near the crack is high enough, dislocations are created near the crack tip. The internal stresses generated by dislocations emitted from the crack tip can harmonize the stress intensity provided by the applied load, which in turn produces toughness in the material. During the processing and use of metal materials, hydrogen gas, known as hydrogen clusters, inevitably enters, which has a serious impact on the mechanical properties of the material. In many real-life situations, such as petrochemicals and aerospace, hydrogen embrittlement is much more common and often results in serious accidents.

After the phenomenon of hydrogen embrittlement was first discovered by Johnson [4] in 1874, it has triggered the enthusiasm of many scholars to study the phenomenon, and then found that the phenomenon of hydrogen-induced embrittlement is universal. Robertson [5] proposed more detailed hydrogen embrittlement mechanism. On the basis of hydrogen embrittlement mechanism, Oriani, Hirth et al [6-13] conducted a detailed study of hydrogen embrittlement phenomenon in iron, and different high strength metallic materials, etc. Tabata and Birnbaum [14] experimentally observed the effect of hydrogen on the velocity of dislocation motion and proposed a theory of hydrogen-enhanced localized plasticity. This theory states that hydrogen increases the rate of motion of dislocations under stress, thus affecting the plasticity and toughness of the material. Sirois [15] proposed the mechanism of hydrogen around dislocations and other elastic stress field centers to explain the effect of hydrogen on dislocation motion. Song [16-17] and others proposed a model of hydrogen clusters consisting of hydrogen atoms aggregated near the crack tip and found that hydrogen hinders dislocation emission at the microscopic crack tip, which in turn hinders blunting and ductile fracture at the crack tip, thus promoting crack tip brittle fracture. Yang [18] proposed a coupled mechanical diffusion model to describe the effect of stress on hydrogen diffusion in titanium. Huynh [19] characterized the microscopic features of hydrogen-induced delayed crack extension in thin plates of single-crystal Fe-3wt % Si alloys.

As technology advances, computer simulations are used to conduct research, which can provide microscopic resolution that cannot be achieved by experiments at the current techniques. Wang and Nowak [20-21] investigated the effect of hydrogen on the dislocation motion of surface single-crystal Fe by nanoindentation experiments and discrete dislocation dynamics simulations. There are several papers [22-25] that investigated the effect of hydrogen on the emission mechanism of α-Fe dislocations using methods such as molecular dynamics simulations and atom modeling. Zhao [26] utilized a molecular dynamics simulation method to investigate the emission of crack tip dislocations in Ni single and crystalline samples in a hydrogen environment. Chen [27] systematically investigated the quantitative characterization of hydrogen-influenced interactions between dislocations and grain boundaries through molecular dynamics simulations. On this basis, Charles [28] predicted hydrogen concentration for various boundary value problems through finite element simulation modeling.

Liu [29] developed a theoretical method for calculating the

stress intensity factors (SIFs) of branching cracks. An asymptotic approximation of the conformal mapping was proposed by employing the Schwarz-Christoffel mapping and Muskhelishvili's method, which was able to derive the critical stress intensity factors for arbitrary branching cracks. Also, the convenience of this analytical method in obtaining SIFs for bifurcated cracks and four-branch cracks is further demonstrated. The interaction between dislocations and cracks and hydrogen clusters has been studied overwhelmingly as a separate study of dislocations and cracks or dislocations and hydrogen clusters. But in reality, all three phenomena often co-exist and interact with each other. Therefore, it is particularly important to investigate the mechanism of hydrogen clusters' effects on dislocation emission from crack tips in nano-metallic bi-materials and explore their impact on the toughness of nanometallic materials.

So this paper is dedicated to study the effect of hydrogen clusters on dislocation emission from interfacial co-linear crack tips in nanometallic materials. Based on the observed results, a theoretical mechanical model to describe the interaction between dislocations emission and hydrogen clusters near an interfacial co-linear crack tip in nano-metallic materials is established and the analytical solution of the model can be obtained through the complex variable method of elasticity. Finally, the effects of hydrogen concentration, temperature, and crack length on the intensity factor of dislocation emission stress at the tip of interfacial co-linear linear cracks are discussed. These discussions contribute to a deeper understanding of the toughening mechanism of nanometallic materials and inform the design and application of this material.

2. Establishment of the Theoretical Model

When hydrogen seeps into metals, it causes a variety of reactions that make the material more vulnerable to failure. In metallic systems such as high-strength steels and nickel, the presence of hydrogen often embrittles the material by causing a sharp transition from ductile fracture (i.e. micro-void coalescence) to brittle intergranular fracture, accompanied by a drastic loss in toughness and ductility. At the microscopic level, when the temperature and strain rate are kept in a certain range, the presence of hydrogen in the solid solution decreases the barrier of dislocation emission, which leads to greater deformation in the local area near the fracture surface. In addition, hydrogen embrittlement occurs mainly at the atomic level, and to investigate the properties of hydrogen embrittlement more easily, we introduced a hydrogen cluster.

As shown in Fig.1, he nanometallic material is a homogeneous and isotropic elastic medium. Under this assumption, the mechanical properties of the material can be described by its shear modulus μ and Poisson's ratio v. The nano-metallic material contains an internal crack consisting of the main crack and its finite-length branch cracks, with the length of the main crack set to be a, the length of the branch cracks set to be b, and the angle between the two cracks set to be $(1\text{-}m)\times\pi$. The material is subjected to far-field type I and type II loads. For the sake of generality, the branch crack length is assumed to be equal to or less than the main crack length, i.e., $b \leqslant a$. Then, introduce a polar coordinate system (r_d, θ), where right endpoint of crack L_0 is set as the origin. An edge dislocation with Burgers vector $b_1 = b_x - ib_y$ is emitted from the co-linear crack interface to the point Z_0. At the same time, a circular hydrogen cluster with a dislocation as the center is generated near the tip of the interface crack, with a radius of $R = 20b_r$. Another polar coordinate system (r_1, φ) is established based on the position of the dislocation, i.e. the center of the circle, as the coordinate origin. In order to study the effect of hydrogen clusters on dislocations, a micro-element area dS is taken from the circular hydrogen cluster at any point.

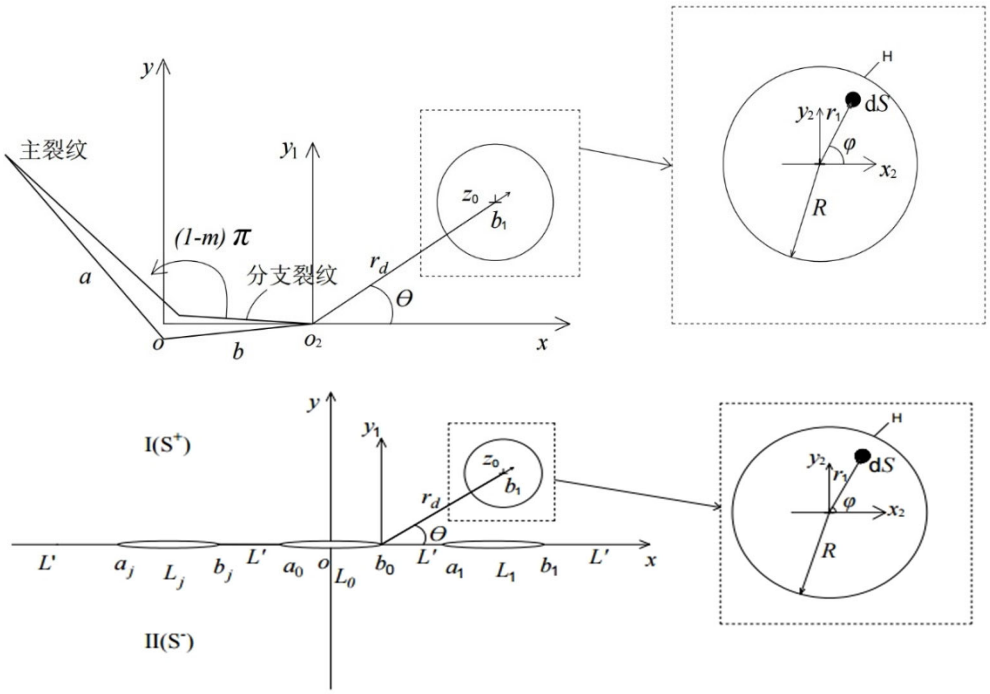

Figure 1. Mechanical model for the interference between hydrogen clusters and dislocation emissions at the tip of a bifurcated crack

3. Derivation of Theoretical Solutions

For plane strain problems, the stress field can be expressed using two of Muskhelishvili's complex potential functions [30]:

$$\begin{cases} \sigma_{xx}+\sigma_{yy}=2\left[\varphi'(z)+\overline{\varphi'(z)}\right] \\ \sigma_{yy}-i\sigma_{xy}=\varphi'(z)+\overline{\varphi'(z)}+\overline{z\varphi''(z)}+\overline{\psi'(z)} \end{cases} \quad (1)$$

Assuming the crack face is free, the boundary conditions for the crack face can be denoted as:

$$\sigma_{yy}(t)-\mathrm{i}\sigma_{xy}(t)=0\text{ , t}\in\text{Blunt crack surface} \quad (2)$$

To solve the problem more easily, the following mapping function is introduced [31]:

$$z=\omega(\zeta)=2R(1+\cos\alpha)e^{i\pi(1-m)}\times\frac{(\zeta-\tan\frac{\alpha}{2})^{1-m}(\zeta+\tan\frac{\alpha}{2})^{1-m}}{\zeta^2+1} \quad (3)$$

Where, $\zeta=\eta+i\zeta$.

Using Eq. (3), the surrounding domain of the crack in the z-plane is mapped to the plane. In addition, $a=4R\left[\cos\left(\frac{\alpha+\beta}{2}\right)\right]^{1+m}\left[\cos\left(\frac{\alpha-\beta}{2}\right)\right]^{1+m}$,

$b=4R\left[\sin\left(\frac{\alpha+\beta}{2}\right)\right]^{1+m}\left[\sin\left(\frac{\alpha-\beta}{2}\right)\right]^{1+m}$ （ b≤a ） ,

$\sin\beta=m\sin\alpha$ (0≤m≤1). The parameters α and β can be determined by assigning values to the factor m and the length b/a.

Derivation of equation (3) gives:

$$z'=\omega'(\zeta)=\frac{2R(1+\cos\alpha)e^{i\pi(1-m)}(1+\cos\alpha)(\zeta-\tan\frac{\alpha}{2})^{m}(\zeta+\tan\frac{\alpha}{2})^{1-m}}{\zeta^2+1}$$

$$-\frac{4R\zeta e^{i\pi(1-m)}(1+\cos\alpha)(\zeta-\tan\frac{\alpha}{2})^{1+m}(\zeta+\tan\frac{\alpha}{2})^{1-m}}{\left(\zeta^2+1\right)^2}$$

$$+\frac{2R(1-m)e^{i\pi(1-m)}(1+\cos\alpha)(\zeta-\tan\frac{\alpha}{2})^{1+m}(\zeta+\tan\frac{\alpha}{2})^{-m}}{\left(\zeta^2+1\right)^2}$$

$$=-\frac{1}{\left(\zeta^2+1\right)^2}[4R\zeta e^{i\pi(1-m)}(1+\cos\alpha)(\zeta-\tan\frac{\alpha}{2})^{m}(\zeta+\tan\frac{\alpha}{2})^{-m}$$

$$\times(\zeta+\tan\frac{\alpha}{2}(m+m\zeta^2+m\tan\frac{\alpha}{2}))] \quad (4)$$

$$z''=\omega''(\zeta)=-\frac{1}{(\zeta^2+1)^3}[-4m\zeta(\zeta^2+1)\tan(\frac{\alpha}{2})^3+(1-3\zeta^2)\tan(\frac{\alpha}{2})^4)$$

$$+2m\zeta(\zeta^4-1)\tan\frac{\alpha}{2}-(-1+4\zeta^2-3\zeta^4+2m^2(1+\zeta^2)^2)\tan(\frac{\alpha}{2})^2$$

$$+4e^{i\pi(1-m)}\mathrm{R}(1+\cos\alpha)(\zeta-\tan\frac{\alpha}{2})^{-1+m}(\zeta+\tan\frac{\alpha}{2})^{-1-m}(\zeta^2(-1+3\zeta^2))] \quad (5)$$

The elastic stress field generated by the emission of dislocations from the bifurcation crack tip can be accurately expressed by the complex potential function and as:

$$\varphi_e(\zeta)=\varphi_{e0}(\zeta)+\varphi_e^*(\zeta) \quad (6)$$

$$\psi_e(\zeta)=\psi_{e0}(\zeta)+\psi_e^*(\zeta) \quad (7)$$

where, $\varphi_{e0}(\zeta)=\bar{\gamma}\ln(\zeta-\zeta_0)-\gamma H/(\zeta-\zeta_0)$,

$\gamma=\mu(b_y-ib_x)/[4\pi(1-\nu)]$,

$\psi_{e0}(\zeta)=\gamma\ln(\zeta-\zeta_0)$, $H=\overline{\omega(\zeta_0)}/\omega'(\zeta_0)$ 。

The complex potential function can be derived as follows:

$$\varphi_e(\zeta)=\gamma\ln(\zeta-\zeta_0)-\frac{\overline{\gamma W}}{\zeta-\overline{\zeta_0}}-\gamma\ln(-\zeta-\overline{\zeta_0}) \quad (8)$$

$$\psi_e(\zeta)=\bar{\gamma}\ln(\zeta-\zeta_0)-\frac{\gamma H}{\zeta-\zeta_0}-\bar{\gamma}\ln(\zeta-\overline{\zeta_0})$$

$$+\frac{\overline{\omega}(\zeta)}{\omega'(\zeta)}[\frac{\gamma}{\zeta-\overline{\zeta_0}}-\frac{\overline{\gamma W}}{(\zeta-\overline{\zeta_0})^2}] \quad (9)$$

where, $W=[\overline{\omega}(\zeta_0)-\overline{\omega(\zeta_0)}]/\omega'(\zeta_0)$.

The force acting on the dislocation at the crack tip consists of three main components: firstly, the dislocation's own like force, which is an internal force generated by the dislocation's own structure; secondly, the force induced by the hydrogen cluster, which is a force exerted on the dislocation by some mechanism due to the presence of hydrogen clusters in the vicinity of the crack tip; and lastly, the force generated by the applied load, which is a force generated by the externally applied mechanical loads transferred through the crack tip to the dislocations.

Firstly, the image force f_d acting on the dislocation itself is calculated. The image force acting on the dislocation is obtained according to the Peach-Koehler formula while considering Eq. (6)-(9):

$$f_d=f_{xe}-\mathrm{i}f_{ye}=\left[\hat{\sigma}_{xy}(\zeta_0)b_x+\hat{\sigma}_{yy}(\zeta_0)b_y\right]+\mathrm{i}\left[\hat{\sigma}_{xx}(\zeta_0)b_x+\hat{\sigma}_{xy}(\zeta_0)b_y\right]$$

$$=\frac{\mu}{4\pi(1-\nu)}\left[\frac{\Phi_e^*(\zeta_0)+\overline{\Phi_e^*(\zeta_0)}}{\gamma}+\frac{\overline{\omega(\zeta_0)}\Phi_e^{*'}(\zeta_0)+\Psi_e^*(\zeta_0)}{\bar{\gamma}}\right] \quad (10)$$

where, $\hat{\sigma}_{xy}$, $\hat{\sigma}_{yy}$ and $\hat{\sigma}_{xx}$ are the perturbation stress components, $\Phi_e^*(\zeta_0)=\varphi_e^{*'}(\zeta_0)/\omega'(\zeta_0)$ and $\Psi_e^*(\zeta_0)=\psi_e^{*'}(\zeta_0)/\omega'(\zeta_0)$.

Then, the force f_h induced by the hydrogen cluster is calculated. As a result of this elastic interaction, the concentration of hydrogen is described by [32]:

$$c_h = 1 + \frac{c_0}{1-c_0}\exp(-\frac{W_{int}}{kT}) \tag{11}$$

where c_h is the hydrogen concentration near the dislocation core, c_0 is the hydrogen concentration in the absence of applied stress; k is the Pozierman constant, and T is the absolute temperature. W_{int} is the interaction energy between the hydrogen cluster and the dislocation in a semi-infinite plane, which can be expressed as [32]:

$$W_{int} = -\frac{\mu b_r(1+\nu)\sin\varphi}{3\pi(1-\nu)r_1}\Delta\upsilon \tag{12}$$

where b_r is the Burgers vector, φ is the angle between the coordinate axis x_2 and the position vector, and r_1 is the distance from the center of the dislocation to the center of the micro-element $\mathrm{d}S$.

Therefore, in polar coordinates, the stress induced by a hydrogen cluster is given by the following equation:

$$f_h = b_r\tau_h = -\frac{\mu b_r\Omega}{2\pi(1-\nu)}\int_{r_2}^{\mathrm{R}}\int_0^{2\pi} c_h sin\frac{2\varphi}{r}\mathrm{d}\varphi\mathrm{d}r \tag{13}$$

where Ω is the partial molar volume and r_2 is the dislocation core radius of the dislocation. During the analysis, it is assumed that the dislocation core radius is equal to the Burgers vector b_r, R is the radius of the hydrogen cluster with the dislocation as the center of the circle.

Finally, the force acting on the edge dislocations due to the applied loads is:

$$f_\Gamma = b_r\tau_a = \frac{b_r K_{\mathrm{I}}^N}{\sqrt{2\pi r_0}}(\frac{1}{2}\sin\frac{\theta}{2}\cos\frac{\theta}{2}) + \frac{b_r K_{\mathrm{II}}^N}{\sqrt{2\pi r_0}}\left(\cos\frac{3\theta}{2} + \sin^2\frac{\theta}{2}\cos\frac{\theta}{2}\right) \tag{14}$$

where $K_{\mathrm{IC}}^{\mathrm{N}}$ and $K_{\mathrm{IIC}}^{\mathrm{N}}$ correspond to model I and model II critical stress intensity factors.

Thus, combining Eqs. (13), (16), and (17), the combined force acting on the dislocation emitted from the tip of the colinear linear crack can be obtained as:

$$f_{emit} = (f_x\cos\theta + f_y\sin\theta) + f_\Gamma = \mathrm{Re}[f_d + f_h]\cos\theta - \mathrm{Im}[f_d + f_h]\sin\theta + f_\Gamma \tag{15}$$

4. Discussion and Analysis

We adopt the generally accepted criterion for dislocation emission. The condition for dislocation emission from crack tips is that the sum of all forces acting on dislocations is zero, and the distance between dislocations and cracks should be greater than the dislocation core radius [38]:

Combining Eq. (15) and the dislocation emission condition $f_{emit} = 0$, the critical stress intensity factor for dislocation emission can be calculated as:

$$K_{\mathrm{I}}^{\mathrm{N}} = 0 \quad ,$$

$$K_{\mathrm{I}}^{\mathrm{N}} = \frac{2\sqrt{2\pi r_0}}{b_r\sin\frac{\theta}{2}\cos\frac{\theta}{2}}(\mathrm{Im}[f_d + f_h]\sin\theta - \mathrm{Re}[f_d + f_h]\cos\theta) \tag{16}$$

$$K_{\Pi}^{\mathrm{N}} = 0,$$

$$K_{\Pi}^{\mathrm{N}} = \frac{\sqrt{2\pi r_0}}{b_r(\cos\frac{3\theta}{2} + \sin^2\frac{\theta}{2}\cos\frac{\theta}{2})}(\mathrm{Im}[f_d + f_h]\sin\theta - \mathrm{Re}[f_d + f_h]\cos\theta) \tag{17}$$

Eqs. (16-17) can be used to analyze the effect of hydrogen clusters on the critical stress intensity factor for dislocation emission from the colinear crack tip. To facilitate the analysis, we dimensionless the stress intensity factors $K_{\mathrm{IC}}^{\mathrm{N}}$ and $K_{\mathrm{IIC}}^{\mathrm{N}}$ as $K_{\mathrm{IC}}^0 = K_{\mathrm{IC}}^{\mathrm{N}} / \mu\sqrt{b_r}$ and $K_{\mathrm{IIC}}^0 = K_{\mathrm{IIC}}^{\mathrm{N}} / \mu\sqrt{b_r}$, respectively. The material parameters of the nanometallic material Ni are used for the lower half plane of the crack, with relative shear modulus $\mu_2 = 73\,\mathrm{Gpa}$, poisson's ratio ν2=0.31. In addition, the Burgers vector b_r =0.25nm is assumed for edge dislocation. The hydrogen-related parameters are set as $\Omega = 3.39\text{Å}^3$, $r_2 = b_r$ and R=20b_r.

As shown in Fig. 2: when θ = 0.5 rad, T = 200 °C, b/a = 0.3, m = 1/3, and C0 = 0.01 mol, the graphs depicting the changing patterns of the two SIFs with the relative position of the hydrogen cluster to the crack tip are shown. From the figure, it can be seen that as the relative position of the hydrogen cluster to the crack tip increases, K_{IC}^0 and K_{IIC}^0 then decreases, so that the hydrogen cluster relatively closer to the bifurcation crack tip hinders the emission of dislocations. When the relative position is certain, $K_{\mathrm{IC}}^0 > K_{\mathrm{IIC}}^0$, indicating that the type II applied load is more likely to emit dislocations from the crack tip than type I. The relative position of the hydrogen cluster to the crack tip increases with the increase of the relative position of the hydrogen cluster to the crack tip.

As shown in Fig.3, the two dimensionless critical SIFs corresponding to the blade-type dislocation emission vary with the temperature T when θ = 0.5 rad, b/a = 0.3, and C_0 = 0.01 mol. As can be seen from the figure, the critical stress intensity factor increases with increasing temperature under the influence of the hydrogen mass, so that the increase in temperature hinders the emission of cleavage-tip dislocations, which leads to a decrease in the toughness of the material induced by the dislocation emission. When the temperature takes a certain value, with the increase of m, the critical stress intensity factor decreases, that is, when the angle between the main crack and the bifurcation crack increases, the tendency of dislocations to be launched from the tip of the bifurcation crack will be more obviously and easily, and the selection of a suitable angle helps the launch of dislocations at the tip of the crack, which improves the toughness of the material due to the launch of dislocations.

As shown in Fig. 4, the variation of the dimensionless critical SIF corresponding to the edge dislocation emission with the hydrogen concentration C_0 is plotted when θ=0.5 rad, T=200°C, and b/a=0.3. From the figure, it can be seen that when different values of m are taken, the critical SIF decreases with the increase of hydrogen concentration, i.e.,

the relatively high hydrogen concentration can promote the emission of dislocations at the crack tip. The critical SIF decreases with the increase of m when the hydrogen concentration takes a certain value, that is, the larger the angle between the main crack and the bifurcation crack, the easier the dislocations at the tip of the bifurcation crack will be emitted.

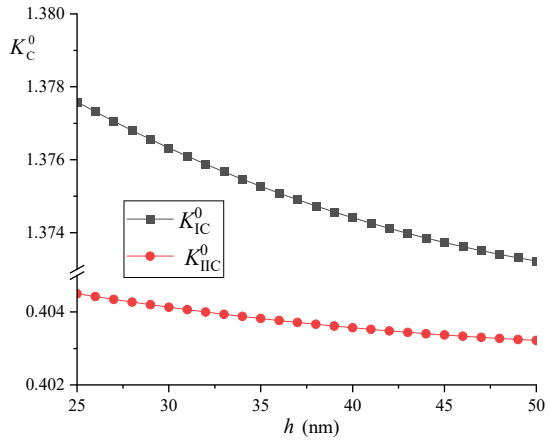

Figure 2. Dependence of normalized critical SIFs with different hydrogen cluster relative position to the fracture tip

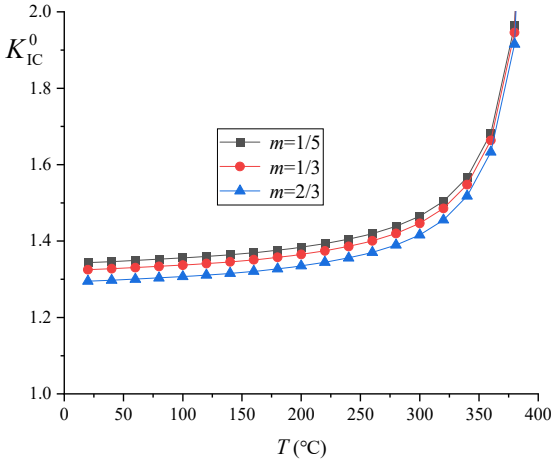

Figure 3. Dependence of normalized critical SIFs on the temperatures T with different m values

As shown in Fig. 5: a plot of the dimensionless SIF of the edge dislocation emission as a function of temperature T when C_0 = 0.01 mol, θ = 0.5 rad, and m = 1/3. increases with increasing temperature. This implies that the emission of cleavage-tip dislocations is hindered in a high temperature environment. When the temperature takes a certain value, the dislocation emission from the bifurcated crack tip becomes progressively more difficult as the relative crack length continues to increase, making it more difficult.

As shown in Fig. 6, when C_0 = 0.01 mol, T = 200 °C, and m = 1/3, the dimensionless two SIFs of the edge dislocation emission vary with the dislocation emission angle θ. As can be seen from Fig. (a), with the increase of the blade dislocation emission angle, it decreases and then increases, and there is a very small value (i.e., the easiest dislocation emission angle θ_{min}). When the relative crack length is taken as b/a=0.2, 0.3, 0.5, 0.7 and 0.9, the corresponding dislocation easiest firing angle is θ_{min} =1.1 rad; and when the dislocation firing angle is taken as a certain value, it increases with the increase of temperature, which leads to more difficult emitting of crack tip dislocations, and thus reduces the toughness of the material due to dislocation emitting.

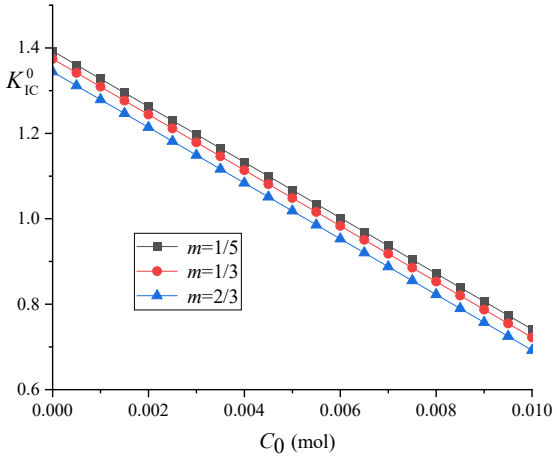

Figure 4. Dependence of normalized critical SIFs on the hydrogen concentrations C0 with different m values

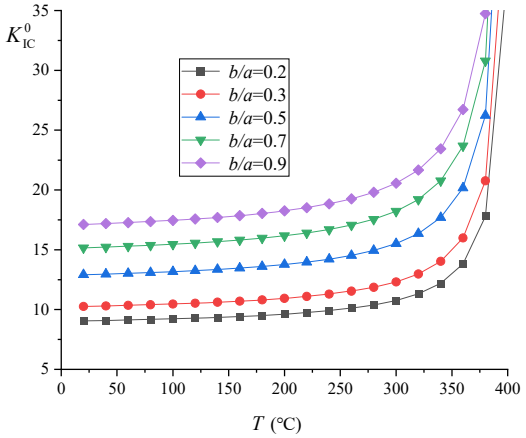

Figure 5. Dependence of normalized critical SIFs on the temperatures T with Different relative crack lengths b/a

As can be seen from Fig. 6(b), the dislocation emission angle of a finite positive value starts to increase rapidly until it tends to infinity, and then becomes negative. When negative dislocations are considered, the absolute value of negative SIF shows a tendency to decrease and then increase with the increase of the dislocation emitting angle, and there also exists an easiest emitting angle for negative dislocations. When the relative crack lengths are taken as b/a=0.3, 0.5, 0.7 and 0.9, the most probable emitting angles of the most corresponding dislocations are θ_{min} =2.0 rad; and when b/a=0.2, θ_{min} =1.8 rad.

As shown in Fig. 7, when C_0=0.01mol, T=200℃, b/a=0.3, the dimensionless two SIFs of the edge dislocation emission are plotted with the change of the dislocation emission angle θ. The SIFs of the edge dislocation emission are shown in Fig. 7. From Fig. 7(a), it can be seen that with the increase of the blade dislocation emission angle, followed by the first decrease and then increase, so there exists an easiest dislocation emission angle. When taking m=1/5, 1/3, and 2/3 respectively, the corresponding easiest dislocation launch angle is θ_{min}=1.4 rad; and when the dislocation launch angle is certain, it decreases with the increase of m, i.e., the larger the angle between the main crack and the bifurcation crack, the easier it is to emission dislocations from the tip of the bifurcation crack, which improves the toughness of the material induced by the dislocation emission.

From Fig. 7(b), it can be seen that the increase of the

dislocation emission angle starts from some finite positive value, then increases rapidly until it tends to infinity, and then becomes negative. Therefore, the most probable dislocation emission angle for a positive edge dislocation is θ_{min}=0 rad. Considering the negative dislocations, the most probable emission angle for the negative dislocations is θ_{min}=1.6 rad for m=1/5, 1/3, and 2/3. For a certain dislocation emission angle, the emission angle decreases with the increase of m. The dislocation emission angle of a positive edge dislocation is θ_{min}=1.6 rad.

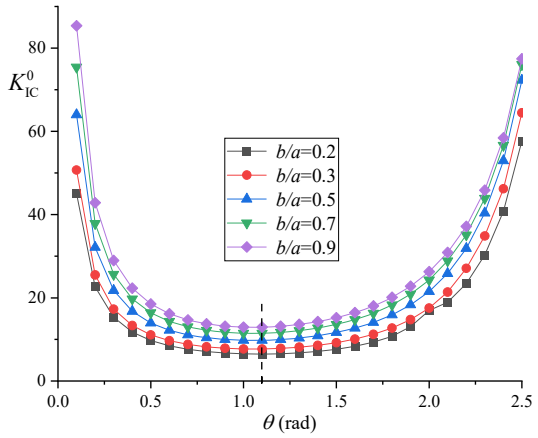

(a) K^0_{IC}

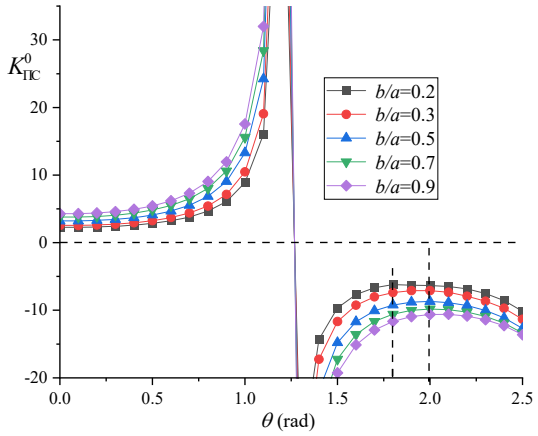

(b) K^0_{IIC}

Figure 6. Dependence of normalized critical SIFs on the emission angle θ with different relative crack lengths b/a for (a) K^0_{IC} ,(b) K^0_{IIC}

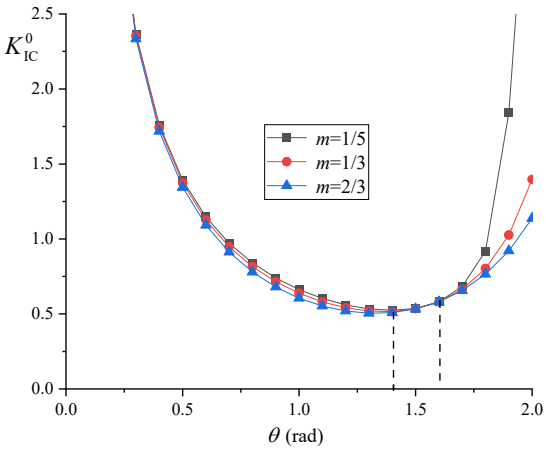

(a) K^0_{IC}

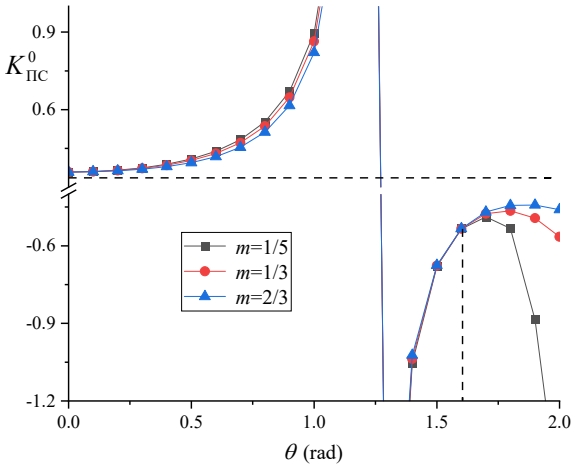

(b) K^0_{IIC}

Figure 7. Dependence of normalized critical SIFs on the emission angle θ with different m values (a) K^0_{IC} , (b) K^0_{IIC}

5. Conclusion

A theoretical model is established to investigate the interaction between the hydrogen clusters and edge dislocation near an bifurcation crack tip in nano-metallic bi-materials. The analytic expression of critical SIFs corresponding to dislocation emission is deduced by the complex potential method in elasticity, and the effect of the hydrogen concentration, temperature, relative crack length, the angle between the main crack and the bifurcation crack and emission angle on the critical SIFs are discussed. The conclusions are summarized as follows:

(1) With the concentration of the applied hydrogen cluster changes, the SIFs under applied loading all decrease with increasing hydrogen concentration. Therefore, dislocations at high hydrogen concentrations are more likely to emit from crack tips.

(2) As the relative crack length increases, dislocation emission from the crack tip is hindered. At the same time, the increase in temperature is also unfavorable to the edge dislocation emission, i.e., high temperatures inhibit the emission of dislocations from the bifurcation crack tip under the influence of hydrogen gas clusters.

(3) The critical SIF under both applied loads decreases with the increase of the angle between the main crack and the bifurcation crack, so the larger the angle is the more favorable for the dislocations to be emitted from the bifurcation crack tip.

References

[1] Abrikosov A. Fundamentals of the Theory of Metals. Phys. Today. Vol. 43 (1990) No. 11, p73-76.

[2] M. S. Muhd Norhasri, M. S. Hamidah, A. Mohd Fadzil. Applications of using nanomaterial in concrete: A review. Constr. Build. Mater. Vol. 133 (2017), p91-97.

[3] Meyers M A, Mishra A, Benson D J. Mechanical properties of nanocrystalline materials. Prog. Mater. Sci. Vol. 51 (2006), p427-556.

[4] Johnson W.H. On some remarkable changes produced in iron and steel by the action of hydrogen and acids. Proc. R. Soc. London. Vol. 23 (1874). No. p156-163, p168-179.

[5] Robertson M I, Sofronis P, Nagao A, et al. Hydrogen Embrittlement Understood. Metall. Mater. Trans. B. Vol.46 (2015) No. 6, p2323.

[6] Oriani R A. Hydrogen embrittlement of steels. Annu. Rev. Mater. Sci. Vol. 8(1978), p327.

[7] Hirth J P. Effects of hydrogen on the properties of iron and steel. Metall. Trans. 11A, Vol. 861 (1980).

[8] Venezuela J, Liu Q, Zhang M, et al. A review of hydrogen embrittlement of martensitic advanced high-strength steels. Corros. Rev. Vol.34 (2016) No. 3, p153-186.

[9] Koyama M, Akiyama E, Lee Y, et al. Overview of Hydrogen Embrittlement in High-Mn Steels. Int. J. Hydrogen Energy. Vol. 42 (2017) No. 17, p12706.

[10] Panday G A. Hydrogen induced cracking of pipeline and pressure vessel steels: A review. Eng. Fract. Mech. Vol. 199 (2018), p609.

[11] Ohaeri E, Eduok U, Szpunar J. Hydrogen related degradation in pipeline steel: A review. Int. J. Hydrogen Energy. Vol. 43 (2018) No. 31, p14584.

[12] Liu Q, Atrens A. A critical review of the influence of hydrogen on the mechanical properties of medium-strength steels. Corros. Rev. Vol. 31 (2013) No.3-6, p85-103.

[13] Dwivedi S K, Vishwakarma M. Effect of hydrogen in advanced high strength steel materials. Int. J. Hydrogen Energy. Vol. 44(2019) No.51, p28007-28030.

[14] Tabata T, Birnbaum H K. Direct observations of hydrogen enhanced crack propagation in iron. Scr. Metall. Vol. 18 (1984) No. 3, p231-236.

[15] Sirois. Effects of hydrogen and carbon on thermally activated deformation in nickel. Acta Metall. Mater. Vol. 40 (1992) No.6, p1377-1385.

[16] Song J, Curtin W A. A nanoscale mechanism of hydrogen embrittlement in metals. Acta Mater. Vol.59 (2011) No.4, p1557-1569.

[17] Song J, Curtin W A. Atomic mechanism and prediction of hydrogen embrittlement in iron. Nat. Mater. Vol. 12 (2013) No. 2, p145-151.

[18] Yang F Q, Zhan W J, Yan T, et al. Numerical Analysis of the Coupling between Hydrogen Diffusion and Mechanical Behavior near the Crack Tip of Titanium. Math. Probl. Eng. Vol. 2020 (2020), p1-15.

[19] Huynh T T, Koyama M, Takahashi Y, et al. Plastic deformation sequence and strain gradient characteristics of hydrogen-induced delayed crack propagation in single-crystalline Fe–Si alloy. Scr. Mater. Vol. 178 (2020), p99-103.

[20] Wang J, Zhao L, Huang M S, et al. Effect of Hydrogen on Dislocation Nucleation and Motion: Nanoindentation Experiment and Discrete Dislocation Dynamics Simulation. Acta Mech. Solida Sin. Vol. 35 (2021) No. 1, p1-14.

[21] Nowak C, Zhou X W. An interplay between a hydrogen atmosphere and dislocation characteristics in BCC Fe from time-averaged molecular dynamics. Phys. Chem. Chem. Phys. Vol. 25 (2023) No. 12, p3290-3299.

[22] Kapci Mehmet Fazil, Schön J. Christian, Bal Burak. The role of hydrogen in the edge dislocation mobility and grain boundary-dislocation interaction in [formula omitted]-Fe. Int. J. Hydrogen Energy. Vol. 46 (2021) No. 64, p32695-32709.

[23] Matsumoto Ryosuke, Oyinbo Sunday T, Mugilgeethan Taketomi Shinya. Hydrogen Effect on the Mobility of Edge Dislocation in α-Iron: A Long-Timescale Molecular Dynamics Simulation. I S I J International. Vol. 62 (2022) No. 11, p 2402-2409.

[24] Xing X, Yu M, Chen W, et al. Atomistic simulation of hydrogen-assisted ductile-to-brittle transition in α-iron. Comput. Mater. Sci. Vol. 127 (2017), p211-221.

[25] Wan L, Geng W T, Ishii A, et al. Hydrogen embrittlement controlled by reaction of dislocation with grain boundary in alpha-iron. Int. J. Plast. Vol. 112 (2019), p206-219.

[26] Zhao K, He J, Zhang Z. Effect of grain boundary on the crack-tip plasticity under hydrogen environment: An atomistic study. J. Appl. Phys. Vol. 127 (2020) No.1, p015101.

[27] Chen J W, Zhu Y X, Huang M S, et al. Study on hydrogen-affected interaction between dislocation and grain boundary by MD simulation. Comput. Mater. Sci. Vol. 196 (2021), p110562.

[28] Charles Yann, Mougenot Jonathan, Gaspérini Monique. Modeling hydrogen dragging by mobile dislocations in finite element simulations. Int. J. Hydrogen Energy. Vol. 47 (2022) No. 28, p13746-13761.

[29] Liu Z-E, Wei Y. A semi-analytical solution to the stress intensity factors of branched cracks[J]. Journal of the Mechanics and Physics of Solids. Vol. 179 (2023), p105351.

[30] Xianghua P, Min Y, Youwen L. Effect of nanotwin and dislocation pileup at twin boundary on dislocation emission from an interfacial collinear crack tip in nanocrystalline materials. Mech. Adv. Mater. Struct. Vol. 27 (2020) No. 12, p965-974.

[31] Muskhelishvili N I. Some Basic Problems of the Mathematical Theory of Elasticity. The American Mathematical Monthly Vol. 74 (1967) No. 6, p752.

[32] Sih G C. Stress Distribution Near Internal Crack Tips for Longitudinal Shear Problems[J]. Journal of Applied Mechanics, Vol. 32 (1965) No.1, p51–58.

[33] Rice J R, Thomson R. Ductile and Brittle Behavior of Crystals. Philos. Mag. Vol. 19(1974) No.1, p73.

[34] P. Sofronis, H.K. Birnbaum. Mechanics of the hydrogen-dislocation-impurity interactions—I. Increasing shear modulus. J. Mech. Phys. Solids. Vol. 43 (1995) No. 1, p49-90.